Chemistry and Materials

The Center for Science Innovation

Research Article

Chem. Mater. 5 (3) 2026, 155-161

Evaluation of the Solution Properties of Binary Mixtures of Dimethyl Sulphoxide and Tetrahydrofuran for Magnesium-Ion Battery Electrolyte

Ngozi Jane Maduelosi*, Okpara Sergeant Bull, Tuakabari Baribeela Nyono

Department of Chemistry, Faculty of Science, Rivers State University, Nkpolu-Oroworukwo P.M.B. 5080, Port Harcourt 500101, Nigeria

*Corresponding author: ngozi.maduelosi@ust.edu.ng

Received
29 July 2026

Received in revised form
21 September 2026

Accepted
23 September 2026

Published online
15 October 2026

DOI
https://doi.org/10.56425/cma.v5i3.146

© 2026 The author(s). Original content from this work may be used under the terms of the Creative Commons Attribution 4.0 International License.

Abstract

This study evaluates the solution properties of binary dimethyl sulphoxide (DMSO)/tetrahydrofuran (THF) mixtures containing magnesium perchlorate ($Mg(ClO_4)_2$) for potential application as magnesium-ion battery electrolytes. Binary DMSO/THF mixtures were prepared over DMSO mole fractions of 1.00, 0.85, 0.75, 0.50, 0.25, 0.15 and 0.00, and measurements were performed from 25 to 55 °C. $Mg(ClO_4)_2$ concentrations of 0.1, 0.5, 1.0 and 2.0 M were investigated. Density, kinematic and dynamic viscosity, as well as electrical/molar conductivity were measured. On the other hand, dielectric constant, critical ion-pair distance, Grunberg–Nissan interaction parameter and excess properties were calculated. Density and viscosity decreased generally with increasing THF fraction and temperature, whereas salt addition increased the viscosity of the electrolyte solutions. The highest reported molar-conductivity value in the supplied dataset was 3.025 S m² mol^{-1} at X_{DMSO} = 0.50 for 1.0 M $Mg(ClO_4)_2$. At 25 °C, the salt-containing mixtures were predominantly negative for excess molar volumes, although small positive deviations occurred at selected compositions and concentrations. Excess viscosity and excess Gibbs free energy of activation also showed composition- and concentration-dependent deviations. The dielectric constant decreased with increasing THF fraction, while the calculated critical distance and Grunberg–Nissan parameter varied with composition. These results indicate that combining DMSO and THF can modify the balance between ion dissociation and mobility, although the optimum composition should be regarded as system-specific.

Keywords: DMSO, tetrahydrofuran, magnesium perchlorate, conductivity, viscosity, excess properties, magnesium-ion battery electrolyte

1. Introduction

Electrolytes control ion transport between electrodes, and strongly influence conductivity, rate capability, temperature response and cycle life in rechargeable batteries [1–5]. Mixed-solvent electrolytes are attractive because a solvent with relatively high dielectric constant can promote salt dissociation, whereas a lower-viscosity co-solvent can facilitate ionic transport [6, 7]. These properties are often difficult to optimize simultaneously in a single solvent [1, 2, 8].

Lithium-ion batteries (LIBs) remain dominant in portable electronics and electric mobility, but their continued large-scale deployment presents several challenges such as limited resource availability of critical raw materials, safety concerns associated with thermal runaway, environmental impacts, high production costs, and difficulties in recycling and end-of-life management [9–12] Lithium supply chains are geographically concentrated: the International Energy Agency reports that the three largest mining countries accounted for 85% of lithium mining in 2023 and the three largest refining countries accounted for 96% of global lithium refining [13].

Such concentration creates exposure to supply disruption and geopolitical risk [13]. LIBs also face safety challenges associated with thermal runaway, which can lead to fire or explosion under severe thermal, electrical or mechanical abuse [14–19]. In addition, current life-cycle assessments identify resource use, environmental impacts, recycling and end-of-life management as continuing sustainability challenges [20–23]. These limitations do not imply that LIBs are unsuitable; rather, they motivate investigation of complementary chemistries that can diversify raw-material supply and provide different safety and performance characteristics.

Rechargeable magnesium-ion batteries (MIBs) are among the post-lithium-ion systems being investigated because magnesium is abundant, divalent and capable of high theoretical volumetric capacity. Recent reviews, however, emphasize that MIB development remains constrained by strong Mg^{2+} interactions, sluggish solid-state diffusion, electrolyte compatibility and passivation at the Mg interface [24–26]. Consequently, electrolyte formulation is a central research problem in the development of magnesium-ion batteries [27–30]. DMSO and THF offer contrasting solvent characteristics that may be exploited through mixing to balance ion dissociation and mobility.

Previous studies of binary organic electrolytes have shown that solvent composition, dielectric response, viscosity and salt concentration can strongly affect conductivity and ion association [31–34]. The present study therefore examines DMSO/THF mixtures containing $Mg(ClO_4)_2$ and evaluates density, viscosity, conductivity, dielectric constant, critical ion-pair distance, Grunberg–Nissan interaction parameter and excess functions.

2. Materials and Method

2.1. Materials and sample preparation

All chemicals were commercially sourced and used without further purification except otherwise. Analytical-grade DMSO (99.5%), THF (95.5%) and dry $Mg(ClO_4)_2$ (99%) were used as reported in the supplied manuscript.

2.2. Sample preparation

Binary mixtures were prepared at DMSO mole fractions of 1.00, 0.85, 0.75, 0.50, 0.25, 0.15 and 0.00. $Mg(ClO_4)_2$ concentrations of 0.1, 0.5, 1.0 and 2.0 M were prepared; the corresponding reported salt masses were 1.117, 5.581, 11.165 and 22.323 g dissolved in 100 cm^3 of the binary mixture. Measurements were made at 25, 35, 45 and 55 °C.

2.3. Measurements

A 20 mL capillary Ostwald viscometer was used for viscosity measurements and calibrated with distilled water at 25 °C. Flow time was measured with an electronic stopwatch (±0.01 s), and measurements were performed in triplicate. Density was determined using a calibrated 10 mL borosilicate-glass pycnometer. Electrical conductivity was measured using a Hanna E-214 conductivity meter after calibration with KCl. Temperature was controlled using a thermostated water bath [35].

2.4. Equations and calculations

Density:

$$\rho = \frac{m}{V} \quad (1)$$

ρ is density, m is sample mass, and V is sample volume.

Kinematic viscosity:

$$v = kt \quad (2)$$

v is kinematic viscosity, k is the viscometer constant, and t is flow time.

Dynamic viscosity:

$$\eta = \rho v \quad (3)$$

η is dynamic viscosity, ρ is density, and v is kinematic viscosity.

Electrical conductivity:

$$\kappa = G\left(\frac{l}{A}\right) = K_{Cell}G \quad (4)$$

κ is electrical conductivity, G is conductance, l is the distance between the electrodes, A is the electrode area, and K_{cell} is the cell constant.

Molar conductivity:

$$\Lambda_m = \frac{\kappa}{C} \quad (5)$$

Λ_m is molar conductivity, κ is electrical conductivity, and C is the molar concentration of the electrolyte in mol m^{-3}. With κ in S m^{-1} and C in mol m^{-3}, Λ_m is in S m^2 mol^{-1}.

Stokes–Einstein relation:

$$D = \frac{k_B T}{6\pi\eta r_D} \quad (6)$$

D is translational diffusion coefficient; k_B is Boltzmann constant; T is absolute temperature; η is dynamic viscosity; r_D is hydrodynamic radius [36].

Dielectric constant of the binary mixture:

$$\varepsilon_{mix} = \frac{\varphi_1\varepsilon_1 + \varphi_2\varepsilon_2}{100} \quad (7)$$

φ_1 and φ_2 are the reported percentage compositions and ε_1 and ε_2 are the dielectric constants of the pure solvents.

Critical ion-pair distance:

$$r = \frac{|z_i z_j| e^2}{8\pi\varepsilon_0\varepsilon_r k_B T} \quad (8)$$

z_i *and* z_j are ion charge numbers; e is elementary charge; ε_o is vacuum permittivity; ε_r *is relative permittivity;* k_B is Boltzmann constant; T is absolute temperature. This is a Bjerrum-type criterion for electrostatic ion pairing [37, 38].

Grunberg–Nissan interaction parameter:

$$d = \frac{[\ln \eta_{mix} - x_1 \ln \eta_1 - x_2 \ln \eta_2]}{x_1 x_2} \quad (9)$$

η_{mix} is mixture viscosity; η_1 and η_2 are pure-component viscosities; x_1 *and* x_2 are mole fractions [39].

Excess molar volume:

$$V^E = \left(\frac{x_1 M_1 + x_2 M_2}{\rho_{mix}}\right) - \frac{x_1 M_1}{\rho_1} - \frac{x_2 M_2}{\rho_2} \quad (10)$$

M_1 and M_2 are molar masses; ρ_{mix} is mixture density; ρ_1 and ρ_2 are pure-component densities.

Excess viscosity:

$$\eta^E = \eta_{mix} - x_1\eta_1 - x_1\eta_1 \quad (11)$$

η^E is the viscosity deviation from the ideal mole-fraction-weighted value.

Excess Gibbs free energy of activation for viscous flow:

$$\Delta G^{*E} = RT[\ln(\eta_{mix} V_{mix}) - x_1 \ln(\eta_1 V_1) - x_2 \ln(\eta_2 V_2)] \quad (12)$$

R is the gas constant, T is absolute temperature, V terms are the corresponding molar volumes.

Redlich–Kister representation:

$$Y^E = x_1 x_2 \sum_{i=1}^{n} A_i (2x_1 - 1)^{i-1} \quad (13)$$

Y^E *represents an excess property and* A_i *are fitted coefficients* [40, 41].

Standard deviation of the fit:

$$\sigma = \left[\frac{\sum (Y^E_{exp} - Y^E_{cal})}{(m-n)}\right]^{\frac{1}{2}} \quad (14)$$

m is the number of experimental points and n is the number of fitted coefficients.

3. Results and Discussion

3.1. Density and viscosity

The measured density decreased systematically as X_{DMSO} decreased from 1.00 to 0.00 (Table 1). At 25 °C, density changed from 1.099 g cm^{-3} for pure DMSO to 0.893 g cm^{-3} for pure THF. The decrease is consistent with the lower density of THF and indicates that composition is a major determinant of the mixture density.

Table 1. Density of DMSO/THF mixtures at 25–55 °C.

X_{DMSO}	25 °C	35 °C	45 °C	55 °C
1.00	1.099	1.095	1.089	1.087
0.85	1.092	1.082	1.071	1.061
0.75	1.069	1.053	1.054	1.044
0.50	1.019	1.008	0.996	0.990
0.25	0.954	0.945	0.951	0.934
0.15	0.918	0.918	0.899	0.897
0.00	0.893	0.888	0.883	0.869

Density also generally decreased with temperature, consistent with thermal expansion and reduced cohesive ordering. Similar composition- and temperature-dependent behaviour has been reported for mixed organic electrolyte systems [31, 32]. The kinematic and dynamic viscosities also decreased as the THF fraction increased (Table 2 and 3), while increasing temperature reduced viscosity. The lower viscosity of THF provides less hydrodynamic resistance to molecular and ionic motion, consistent with the Stokes–Einstein relation [36].

In the salt-containing solutions, the source data show an increase in viscosity with increasing $Mg(ClO_4)_2$ concentration, indicating that ion–solvent interactions and increased solution structuring contribute to the resistance to flow. Comparable concentration effects have been reported for mixed organic electrolytes [33, 34].

Table 2. Kinematic viscosity of DMSO/THF mixtures at 25–55 °C.

X_{DMSO}	25 °C	35 °C	45 °C	55 °C
1.00	1.989	1.876	1.671	1.402
0.85	1.651	1.661	1.489	1.212
0.75	1.211	1.231	1.157	0.976
0.50	0.881	0.867	0.806	0.779
0.25	0.735	0.702	0.682	0.673
0.15	0.669	0.615	0.552	0.552
0.00	0.525	0.499	0.460	0.419
0.15	0.614142	0.564570	0.496258	0.495144
0.00	0.468825	0.443112	0.406180	0.364111

Table 3. Dynamic viscosity of DMSO/THF mixtures at 25–55 °C.

X_{DMSO}	25 °C	35 °C	45 °C	55 °C
1.00	2.188911	2.054220	1.819719	1.523974
0.85	1.802892	1.797202	1.594719	1.285932
0.75	1.294559	1.296243	1.219478	1.018944
0.50	0.897739	0.873936	0.802776	0.771210
0.25	0.701190	0.663390	0.648582	0.628582

3.2. Conductivity and concentration effects

Molar conductivity varied strongly with both solvent composition and $Mg(ClO_4)_2$ concentration (Table 4). The highest reported value in the supplied dataset is 3.025 S m^2 mol^{-1} at X_{DMSO} = 0.50 and 1.0 M $Mg(ClO_4)_2$.

Table 4. Molar conductivity values reported for $Mg(ClO_4)_2$ in DMSO/THF at 25 °C.

X_{DMSO}	0.1 M	0.5 M	1.0 M	2.0 M
1.00	1.290	0.646	1.401	0.858
0.85	1.440	0.656	2.422	2.055
0.75	1.280	0.670	2.399	2.047
0.50	1.920	0.764	3.025	2.090
0.25	1.090	0.476	2.308	2.248
0.15	1.020	0.452	1.832	1.783
0.00	4.100	1.064	0.950	0.690

The maximum at an intermediate composition is consistent with a balance between DMSO-mediated ion dissociation and THF-mediated reduction in viscosity. Related mixed-solvent studies have reported improved conductivity when a high-dielectric solvent is combined with a lower-viscosity co-solvent [31–34]. Increasing salt concentration can increase the number of charge carriers, but the conductivity response is governed by the product

of carrier concentration and ionic mobility. At sufficiently high concentration, stronger ion–ion electrostatic interactions, ion pairing/aggregation and increased viscosity can reduce the fraction and mobility of charge carriers. The observed decline in molar conductivity at 2.0 M relative to the maximum at 1.0 M may be due to the competing carrier concentration and mobility. This interpretation is consistent with Nwokobia *et al.*, who reported that conductivity in $LiClO_4$/PC–DME mixtures depended on salt concentration together with viscosity, dielectric constant and ion–ion/ion–solvent interactions; their lowest concentration (0.1 M) gave the highest molar conductivity in that particular system [33].

3.3. Excess properties

At 25 °C, the excess molar volumes of the salt-containing mixtures are predominantly negative across the interior composition range (Fig. 1).

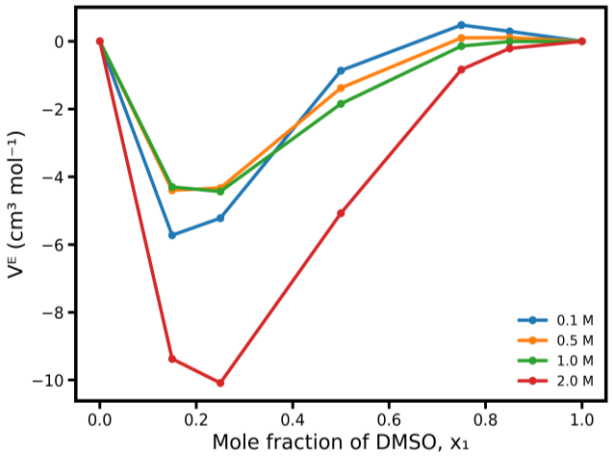

Figure 1. Excess molar volume (V^E) of DMSO/THF mixtures containing $Mg(ClO_4)_2$ at 25 °C.

Negative V^E denotes contraction relative to the ideal volume-additivity reference and is consistent with non-ideal interactions between unlike components. In the DMSO/THF system, the more polar DMSO can participate in strong dipolar interactions, while the ether oxygen of THF provides an electron-rich site; the observed contraction is therefore consistent with specific unlike-molecule interactions and volume additivity. Related excess-volume studies of binary organic mixtures have likewise used the sign and magnitude of V^E as indicators of molecular association [42, 43].

The excess viscosity values (Fig. 2) change sign with composition, temperature and salt concentration rather than remaining uniformly positive. Positive η^E indicates a positive deviation from the ideal mole-fraction-weighted viscosity and is consistent with increased structuring or specific unlike-molecule/solute–solvent interactions; negative η^E indicates the opposite deviation. The concentration dependence supports the view that Mg^{2+} and ClO_4^- alter the local solvent structure and flow resistance [33, 34, 42].

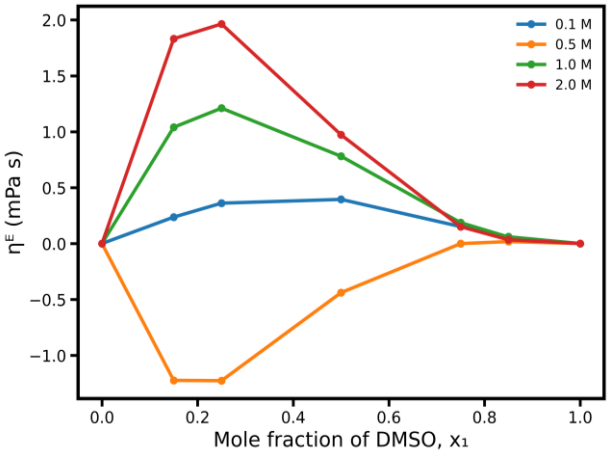

Figure 2. Excess viscosity (η^E) of DMSO/THF mixtures containing $Mg(ClO_4)_2$ at 25 °C.

The excess Gibbs free energy of activation for viscous flow was positive at 25 °C (Fig. 3), indicating positive deviation from ideal solution behaviour and differences in molecular interactions within the mixed solvent.

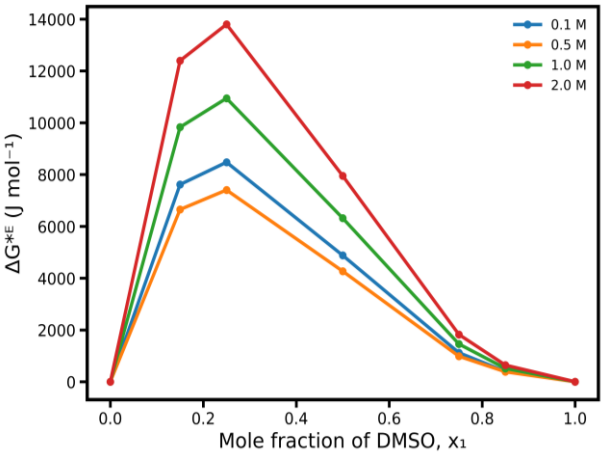

Figure 3. Excess Gibbs free energy of activation for viscous flow (ΔG^{*E}) of DMSO/THF mixtures containing $Mg(ClO_4)_2$ at 25 °C.

3.4 Dielectric constant and critical ion-pair distance

The dielectric constant decreased from 46.83 for DMSO to 7.43 for THF as X_{DMSO} decreased from 1.00 to 0.00 as shown in Fig. 4. This trend is expected from the contrasting polarity of the two solvents. Lower dielectric response reduces electrostatic screening and can favour ion association. The calculated critical distance also varied non-monotonically with composition, with the largest reported value occurring near X_{DMSO} = 0.50. Bjerrum-type ion-pair criteria relate the characteristic association distance to ionic charge, dielectric constant and temperature; therefore, both solvent polarity and temperature must be considered when interpreting the calculated distance [37, 38].

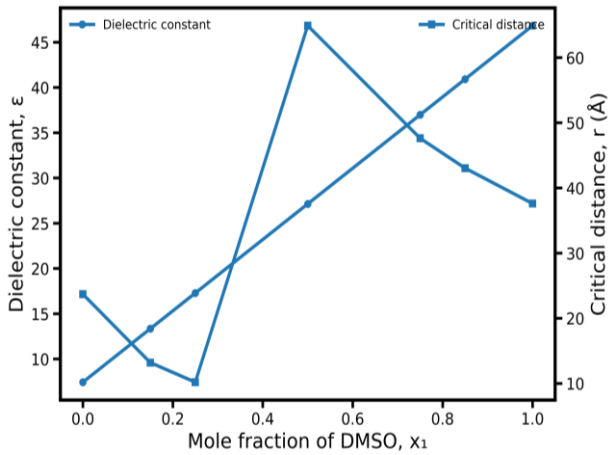

Figure 4. Dielectric constant and critical ion-pair distance of the DMSO/THF system as a function of X_{DMSO}.

3.5 Grunberg–Nissan interaction parameter

The Grunberg–Nissan d parameter changed sign across the composition range (Fig. 5). Positive values indicate a positive deviation from the logarithmic ideal-mixture viscosity relation and are commonly interpreted as stronger unlike-molecule interactions, whereas negative values indicate a negative deviation [39]. The present values therefore support composition-dependent non-ideality rather than a single interaction regime throughout the DMSO/THF system.

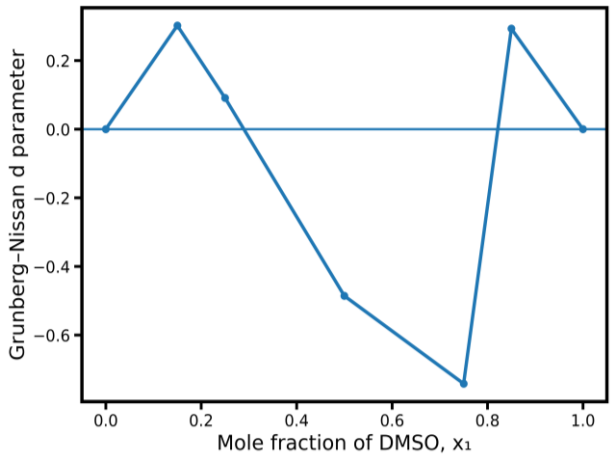

Figure 5. Grunberg–Nissan d parameter of the DMSO/THF system as a function of X_{DMSO}.

4. Conclusion

DMSO/THF mixed solvents containing $Mg(ClO_4)_2$ show composition-dependent density, viscosity, conductivity and excess-property behaviour relevant to electrolyte design. Density and viscosity generally decrease with increasing THF fraction and temperature, while salt addition increases viscosity. The supplied conductivity dataset gives its highest reported molar-conductivity value at X_{DMSO} = 0.50 and 1.0 M $Mg(ClO_4)_2$. The conductivity response at high salt concentration is best explained by competition between the increasing number of charge carriers and reduced mobility arising from ion–ion association, ion pairing and increased viscosity. At 25 °C, salt-containing mixtures show predominantly negative V^E values, while the complete temperature-dependent dataset contains sign changes that require verification before a universal statement is made. The dielectric constant decreases with increasing THF fraction, and the Grunberg–Nissan parameter indicates composition-dependent non-ideality. These results support further evaluation of DMSO/THF mixtures as candidate Mg-ion electrolyte media, but cell-level electrochemical testing is required before claiming battery-performance superiority.

Author contributions

Ngozi Jane Maduelosi: Conceptualization, Supervision, Methodology, Validation, Writing – review & editing. **Okpara Sergent Bull**: Supervision, Methodology, Validation, Writing – review & editing. **Tuakabari Baribeela Nyono**: Investigation, Methodology, Data curation, Formal analysis, Writing – original draft.

Conflicts of interest

There are no conflicts to declare

Acknowledgement

The authors appreciate the technical and analytical contributions of Mr. C. M. Ekezie and Mr. B. B. Dume to this research.

References

[1] K. Xu, Nonaqueous liquid electrolytes for lithium-based rechargeable batteries, *Chem. Rev.* **104** (2004) 4303–4418. https://doi.org/10.1021/cr030203g

[2] M. Dahbi, F. Ghamouss, F. Tran-Van, D. Lemordant, M. Anouti, Comparative study of EC/DMC LiTFSI and $LiPF_6$ electrolytes for electrochemical storage, *J. Power Sources* **196** (2011) 9743–9750. https://doi.org/10.1016/j.jpowsour.2011.07.071

[3] R. Tiwari, D. Kumar, D.K. Verma, K. Parwati, P. Rajan, R. Rai, S. Krishnamoorthir R. Khan, Fundamental chemical and pjysical properties of electrolytes in energy storage devices: A rewiew, J. *Energy Storage, 81* (2024) 110361. https://doi.org/10.1016/j.est.2023.110361.

[4] G. Leverick, Y. Shao-Horn, controlling electrolyte properties and redox reactions using solvation and implications in battery functions: A mini-review, *Adv. Energy Materials*, **13** (2023) 220409094. https://doi.org/10.1002/aenm.202204094.

[5] J O'M. Bockris, A.K.N. Reddy, M. Gamboa-Aldeco, Electrocemistry 2A: Fundamentals of Electrodics, 2nd ed, Springer. (2000).

[6] B. Pal, S. Ramesh, V. Thangaduari, R. Jose, Electrolyte

selection for supercapacitive devices: A critical review, *Nanoscale Adv.* **1** (2019) 3807-3853. https://doi.org/10.1039/C9NA00374F.

[7] K.F. Ren, H. Lui, J.X. Guo, X. Sun, F. Jiang, C. Guo, W. Bao, F. Yu, G. Kalimuldina, L. Kong, X.B. Cheng, J. Li, Working principles of high-entropy electrolytes in rechargeable batteries, *ACS energy lett.* **9** (2024) 2960-2980. https://doi.org/10.1021/acsenergylett.4c00621.

[8] C. Don-Lawson, Mixed electrolyte for improved battery system, Direct Res. J. Chem. *Mater. Sci.* **6** (2019) 41–44.

[9] N. Sharmili, R. Nagi, P. Wang, A review of research in the li-ion battery production and reverse suply chain, *J. Energy Storage* **68** (2023) 107622.

[10] Y. Dia, A, Panahi,Thermal runway process in liyhium-ion batteries: A review, *Next Energy* **6** (2025) 1-18 100186.

[11] B.K. Biswal, B. Zhang, P.T.M. Tran, J. Zhang, R. Balasubramanian, Recycling of spent lithiun-ion batteries for sustainable future: recent advancements, *Chem. Soc. Rev.* **53** (2024) 5552-5592.

[12] P.M. Tembo, C. Dyer, V. Subramanian, Lithuim-ion battery recycling-a review of the material supply and policy infrastructure, NPG *Asia Mater.* **16** (2024) 1-20.

[13] International Energy Agency, Lithium, IEA, Paris (2024).

[14] X. Hu, F. Gao, Y. Xiao, D. Wang, Z. Gao, Z. Huang, S. Ren, N. Jiang, S. Wu, Advancements in the safety of lithium-ion battery: The trigger, consequence and mitigation method of thermal runaway, *Chem. Eng. J.* **481** (2024) 148450. https://doi.org/10.1016/j.cej.2023.148450.

[15] Y. Dai, A. Panahi, Thermal runaway process in lithium-ion batteries: A review, *Next Energy* **6** (2025) 100186. https://doi.org/10.1016/j.nxener.2024.100186.

[16] Q. Wang, B. Mao, S.I. Stoliarov, J. Sun, A review of Energy Combust. Lithium-ion battery failure mechanisms and fire prevention strategies. *Prog. Sci*. **73**, (2019) 95–131. https://doi.org/10.1016/j.pecs.2019.03.002.

[17] Y. Chen, Y. Kang, Y. Zhao, L. Wang, J. Liu, Y. Li, Z. Liang, X. He, X. Li, N. Tavajohi, B. Li, A review of lithium-ion battery safety concerns: The issues, strategies, and testing standards. *J. Energy Chem*. **59**, (2021) 83–99. https://doi.org/10.1016/j.jechem.2020.10.017.

[18] J. Jaguemont, F. Bardé, A critical review of lithium-ion battery safety testing and standards. *Appl. Therm. Eng.* **219** (2023) 121014. https://doi.org/10.1016/j.applthermaleng.2023.121014.

[19] T. Shan, P. Zhang, Z. Wang, X. Zhu, Insights into extreme thermal runaway scenarios of lithium-ion batteries fire and explosion: A critical review, *J. Energy Storage*, **88** (2024) 111532. https://doi.org/10.1016/j.est.2024.111532.

[20] J.C. Barbosa, R.S. Pinto, J.P. Serra, C.M. Costa, S. Lanceros-Mendez, R. Gonçalves, Lithium based battery systems: technological and environmental challenges and opportunities, J. *Mater. Chem.* **13** (2025) 35952–35975. https://doi.org/10.1039/D5TA05419B.

[21] A.M. Domingues, R.G. Souza, Review of life cycle assessment on lithium-ion batteries (LIBs) recycling. *Next Sustain*. **3** (2024) 100032. https://doi.org/10.1016/j.nxsust.2024.100032.

[22] Y. Zhou, X.-D. Cui, A.-J. Lin, Y. Dong, G.-L.Duan, Environmental life cycle assessment on the recycling processes of power batteries for new energy vehicles. *J. Clean. Prod.* **488** (2024) 144641. https://doi.org/10.1016/j.jclepro.2024.144641.

[23] Ma, R., Tao, S., Sun, X. Y. Ren, C. Sun, G. Ji, J. Xu, X. Wang, X. Zhang, Q. Wu, G. Zhou, Pathway decisions for reuse and recycling of retired lithium-ion batteries considering economic and environmental functions, *Nat Commun* **15** (2024) 7641. https://doi.org/10.1038/s41467-024-52030.

[24] Y. Man, P. Jaumaux, Y. Xu, Y. Fei, X. Mo, G. Wang, X. Zhou, Research development on electrolytes for magnesium-ion batteries, *Sci. Bull.* **68** (2023) 1819–1842. https://doi.org/10.1016/j.scib.2023.07.027.

[25] Das, N.T.M. Balakrishnan, P. Sreeram, et al., Prospects for magnesium ion batteries: A comprehensive materials review, *Coord. Chem. Rev.* **502** (2024) 215593.

[26] D. Wang, Z. Zhang, Y. Hao, et al., Challenges and progress in rechargeable magnesium-ion batteries: Materials, interfaces, and devices, *Adv. Funct. Mater*. **34** (2024) 2410406. https://doi.org/10.1002/adfm.202410406.

[27] H. Zang, L. Qiao, M. Armand, Organic electrolyte design for rechargeable batteries: From lithium to magnesium, *Angew. Chem. Int. Ed. Engl.* **61** (2022) e202214054.

[28] Y. Sun, F. Ai, Y.-C. Lu, Electrolyte and interphase design for magnesium anode: Major challenges and perspective, *Small* **18** (2022), e2200009.

[29] Q. Sun, S. Luo< R. Huang, S. Yang, X. Lin, Recent progress of magnesium electrolytes for rechargeable magnesium batteries, *Coord. Chem. Rev.* **515** (2024) 215956.

[30] S. Riedel, L. Wang, M. Fitcher, Z. Zhao-Karger, Recent advances in electrolyte for magnesium batteries: Bridging the gap between chemistry and electrochemistry, *Chem. -Eur. J*. **30** (2024).

[31] N.J. Maduelosi, A.A. Abia, F.U. Nwokobia, Characterization of mixed solvents of tetrahydrofuran and acetonitrile for magnesium ion battery, *Chem. Mater. Res.* **6** (2014) 188–193.

[32] A.I. Edimeh, O.A. Ekpete, F. Kpee, Conductivity and viscosities studies of mixed organic electrolyte solvents of propylene carbonate, diethyl carbonate and dimethylformamide for high energy density

lithium-ion and magnesium-ion batteries at 298.15 K, *Int. J. Res. Eng. Sci.* **10** (2022) 62–67.

[33] F.U. Nwokobia, G.A. Cookey, A.A. Abia, The effect of salt concentration on the conductivity and viscosity of binary mixed electrolyte solutions, *IOSR J. Appl. Chem.* **8** (2015) 35–41.

[34] R. Okah, A.A. Abia, G.A. Cookey, N.J. Maduelosi, The study of the intermolecular interactions of mixed solvents of propylene carbonate and dimethylformamide for magnesium ion battery, Chem. Sci. Rev. Lett. **6** (2017) 1711–1715.

[35] N.J. Maduelosi, B.B. Dume, P.M. Amaibi, Investigating the electrical properties and potentials of magnesium-ion electrolyte in binary solvent of propylene carbonate and acetonitrile, *J. Chem. Soc. Niger.* **50** (2025) 554–562.

[36] International Union of Pure and Applied Chemistry, Stokes–Einstein equation, IUPAC Gold Book, 5th ed. (2025). https://doi.org/10.1351/goldbook.12260.

[37] N. Bjerrum, Untersuchungen über Ionenassoziation, *Z. Elektrochem.* **30** (1926) 137–150.

[38] L.O.S. Colbin, Y. Shao, R. Younesi, Ion-pairing: A bygone treatment of electrolyte solutions, *Batteries Supercaps* **8** (2025) 10.1002/batt.202400160.

[39] L. Grunberg, A.H. Nissan, Mixture law for viscosity, *Nature,* **164** (1949) 799–800. https://doi.org/10.1038/164799b0.

[40] O. Redlich, A.T. Kister, Thermodynamics of nonelectrolyte solutions—x-y-t relations in a binary system, *Ind. Eng. Chem.* **40** (1948) 341–345. https://doi.org/10.1021/ie50458a035.

[41] M.L. Singh, Excess properties of binary mixtures of tri–iso-amyl phosphate + n-hexane (or n-dodecane): Physical significance of coefficients of Redlich–Kister type equation, *J. Mol. Liq.* **341** (2021) 117203.

[42] S.I. Orjiocha, M.U. Ibezim-Ezeani, H.O. Abugu, J.O. Ogbodo, J. Akor, A.C. Nwanya, M. Horsfall, Excess parameters of binary mixtures of nitrobenzene–dimethyl sulphoxide (NB–DMSO), *Commun. Phys. Sci.* **8** (2022) 484–492.

[43] C.M. Ekezie, G.A. Cookey, N.J. Maduelosi, Volumetric and viscometric studies of binary mixtures of methanol and some alkyl acetates at varying temperatures, *S. Afr. J. Chem.* **77** (2023) 133–137.